Tensors, non-Gaussianities, and the future of potential reconstruction

Brian A. Powell*
Institute for the Physics and Mathematics of the Universe, University of Tokyo, Kashiwa, Chiba 277-8568, Japan

Konstantinos Tzirakis† and William H. Kinney‡
Dept. of Physics, University at Buffalo, The State University of New York, Buffalo, NY 14260-1500

(Dated: January 15, 2009)

We present projections for reconstruction of the inflationary potential expected from ESA's upcoming Planck Surveyor CMB mission. We focus on the effects that tensor perturbations and the presence of non-Gaussianities have on reconstruction efforts in the context of non-canonical inflation models. We consider potential constraints for different combinations of detection/null-detection of tensors and non-Gaussianities. We perform Markov Chain Monte Carlo and flow analyses on a simulated Planck-precision data set to obtain constraints. We find that a failure to detect non-Gaussianities precludes a successful inversion of the primordial power spectrum, greatly affecting uncertainties, even in the presence of a tensor detection. In the absence of a tensor detection, while unable to determine the energy scale of inflation, an observable level of non-Gaussianities provides correlations between the errors of the potential parameters, suggesting that constraints might be improved for suitable combinations of parameters. Constraints are optimized for a positive detection of both tensors and non-Gaussianities.

I. INTRODUCTION

A faithful reconstruction of the inflaton potential is paramount to understanding the epoch of inflation. Recent cosmological observations [1–5] have revealed much about the possible forms of the potential [6–9]. Future CMB missions, such as ESA's Planck Surveyor [10], and ground-based polarization experiments such as BICEP [11], promise to further hone our understanding of the early universe. The Planck Surveyor will provide improved measurements of the temperature and E-mode polarization anisotropies of the CMB out to $\ell = 3000$, and will detect the B-mode polarization characteristic of gravity waves if the tensor/scalar ratio, r, is greater than around 0.05. Planck will also provide the first high-quality measurement of any departure from Gaussianity exhibited by the CMB temperature fluctuations, with a projected sensitivity $|f_{NL}| \gtrsim 5$ [12, 13].

Recent times have also seen exciting progress in inflationary model building, and much is now understood about how to implement inflation within string theory (see [14–17] for reviews). One particularly exciting realization is provided by the dynamics of D-branes evolving in a higher-dimensional, warped spacetime. A novel aspect of these models is the existence of a speed limit on the field space, resulting from causality restrictions on the motion of the branes in the bulk spacetime. This allows for slow roll to be achieved even in the presence of a steep potential. In terms of effective field theory, the speed limit is enforced by non-canonical kinetic terms in the DBI action describing the motion of the D-branes. These models, termed DBI inflation [18], are further distinguished by the fact that scalar perturbations propagate at a sound speed $c_s \leq 1$. In the limit $c_s \ll 1$, these fluctuations exhibit strong non-Gaussianities [19–23]. Non-Gaussianities of this type were first popularized in the context of *k-inflation* [24], a model-independent construction in which higher-derivative kinetic terms drive inflation in the absence of any potential energy. This phenomenon is a general characteristic of models with non-canonical kinetic terms in the Lagrangian.

With the advent of these more sophisticated theoretical constructions, and the increasingly accurate cosmological probes planned to study them, more generalized methods of inflationary reconstruction have been developed. Bean *et al.* [25] present a formalism for reconstructing a general action – both potential and non-canonical kinetic energy functions can be linked to observations. The new functional degree of freedom presented by the non-canonical form of the kinetic energy typically gives rise to additional observational signatures. For example, the speed of sound, c_s, becomes an additional dynamical degree of freedom in k-inflation and DBI, giving rise to non-Gaussian density fluctuations. However, c_s also affects the form of the primordial power spectra. A successful reconstruction of the inflaton potential, $V(\phi)$, thus requires a measurement of c_s, since otherwise the expressions giving the spectral parameters cannot be uniquely inverted to obtain $V(\phi)$. An accurate reconstruction must also include a detection of the tensor power spectrum. Currently, neither of these quantities have been measured: present bounds on any non-Gaussianities lie within $-9 < f_{NL}^{\rm local} < 111$ and $-151 < f_{NL}^{\rm equil} < 253$ (95% CL) [5], and $r < 0.2$ (95% CL) with WMAP+BAO+SN [5] and $r < 0.35$ (95% CL) for WMAP+ACBAR [26] for power-law spectra, but might

*Electronic address: brian.powell@ipmu.jp
†Electronic address: ct38@buffalo.edu
‡Electronic address: whkinney@buffalo.edu

be larger if more exotic spectra are considered [27].

In this paper, we make reconstruction projections for the Planck satellite within the context of this larger inflationary parameter space, namely, one that contains c_s as an additional degree of freedom. We seek to determine what combination of observations will be required to most successfully reconstruct the potential. In the best of all worlds, future observations will detect both tensors and non-Gaussianities, telling us not only that exotic physics is responsible for inflation, but also allowing for a successful reconstruction program. In this paper, we focus particularly on cases in which only one of these observables is positively detected.

In Section 2, we review potential reconstruction for the case of non-canonical inflation. In Section 3, we perform a Bayesian analysis on a simulated Planck-precision dataset for which there is a positive tensor detection, $r = 0.1$, but no detection of non-Gaussianities, $|f_{NL}| < 5$. This corresponds to a universe in which canonical inflation took place (with $c_s = 1$), or, for example, DBI inflation with $c_s \in [0.25, 1]$. We obtain constraints on $V(\phi_0)$, $V'(\phi_0)$, and $V''(\phi_0)$ for both possibilities and find that the error bars are significantly larger if c_s is taken as a free parameter within the above range. Our inability to resolve c_s prohibits us from using the shape of the power spectra alone to reconstruct $V(\phi)$. In Section 4, we investigate this problem using inflationary flow methods. The flow method is a natural extension of the MCMC analysis, allowing higher dimensional parameter spaces to be explored with relative ease. We reproduce the results obtained in Section 3, and then investigate the effect of allowing the speed of sound to vary over the course of inflation. We find that constraints on V_0'' loosen considerably as this new degree of freedom is introduced. Next, we use flow methods to investigate the observational possibility of a positive detection of f_{NL} and a null detection of r. We find that constraints on the individual potential parameters are worse in this case than in the case where tensors are detected, but that the errors are highly correlated, and tight bounds can be placed on combinations of these parameters. Finally, we consider the case for which *both* r and f_{NL} are measured. This is clearly the best case scenario for near future experiments, since it will not only place bounds on the potential parameters from above and below, but it will also be a smoking gun for exotic physics. In Section 5 we present conclusions.

II. INFLATION MODELS WITH AN ARBITRARY SPEED OF SOUND

A. Flow parameters and reconstruction

In this section we consider the case of a scalar field with a general Lagrangian $\mathcal{L}(X, \phi)$, where ϕ is the field that is responsible for inflation (*the inflaton*) and $X = (1/2)g^{\mu\nu}\partial_\mu\phi\partial_\nu\phi$. If the inflaton field is coupled to Einstein gravity, the total action S can be written [28]

$$S = \int d^4x\sqrt{-g}\left[\frac{1}{2}M_{\rm Pl}^2 R + \mathcal{L}(X,\phi)\right], \qquad (1)$$

where R is the curvature scalar and we work in units of the reduced Planck mass, $M_{\rm Pl} = m_{\rm Pl}/\sqrt{8\pi}$. We can also describe the inflaton field ϕ as a perfect fluid by expressing the energy-momentun tensor $T_\nu{}^\mu$ in the following way

$$T_\nu{}^\mu = (\rho + P)u_\nu u^\mu - P\delta_\nu{}^\mu, \qquad (2)$$

where the pressure P is identified with the Lagrangian $\mathcal{L}(X, \phi)$, ρ is the energy density of the field,

$$\rho = 2X\frac{\partial\mathcal{L}(X,\phi)}{\partial X} - \mathcal{L}(X,\phi) = 2X\mathcal{L}_{,X} - \mathcal{L}, \qquad (3)$$

and

$$u_\nu = \frac{\partial_\nu\phi}{\sqrt{2X}}, \qquad (4)$$

is the fluid 4-velocity. Assuming that the four-dimensional metric is of the Friedmann-Robertson-Walker (FRW) form

$$g_{\mu\nu} = \mathrm{diag}\left(-1, a^2(t), a^2(t), a^2(t)\right), \qquad (5)$$

the Friedmann and the acceleration equations are [25]

$$\begin{aligned} H^2 \equiv \left(\frac{\dot{a}}{a}\right)^2 &= \frac{1}{3M_{\rm Pl}^2}\rho, \\ \frac{\ddot{a}}{a} &= -\frac{1}{6M_{\rm Pl}^2}(\rho + 3P). \end{aligned} \qquad (6)$$

The speed at which fluctuations propagate relative to the homogeneous background is determined by the sound speed of the fluid,

$$c_s^2 \equiv \frac{dP}{d\rho} = \frac{P_{,X}}{P_{,X} + 2XP_{,XX}} = \frac{1}{\gamma^2}. \qquad (7)$$

Inflation models driven by canonical scalar fields satisfy

$$P_{,XX} = 0, \qquad (8)$$

and so fluctuations travel at the speed of light

$$c^2 = 1. \qquad (9)$$

However, in general non-canonical models, fluctuations can propagate at speeds much lower, resulting in non-Gaussian adiabatic fluctuations [19–22]. In terms of the comoving curvature perturbation, ζ, the existence of non-Gaussianities is reflected in a non-trivial three-point function, $\langle\zeta_{\mathbf{k}_1}\zeta_{\mathbf{k}_2}\zeta_{\mathbf{k}_3}\rangle$. In non-canonical models the dominant source of non-Gaussianity is due to configurations for which the wavenumbers $k_1 = k_2 = k_3$, forming equilateral triangles in Fourier space. To lowest order in slow

roll, the magnitude of this non-Guassianity is given by the parameter [20],

$$f_{NL}^{\rm equil} = \frac{35}{108}\left(\frac{1}{c_s^2}-1\right) - \frac{5}{81}\left(\frac{1}{c_s^2}-1-2\Lambda\right), \quad (10)$$

with

$$\Lambda = \frac{X^2P_{,XX} + \frac{2}{3}X^3P_{,XXX}}{XP_{,X} + 2X^2P_{,XX}}. \quad (11)$$

In the context of more general actions such as Eq. (1), the process of reconstructing the physics of inflation requires an understanding of both the potential energy of the field, $V(\phi)$, and the kinetic term. Such a formalism was recently developed in Ref. [25] in terms of different hierarchies of *flow parameters*. Such parameters naturally arise in the Taylor expansions of the functions H, γ, and $\mathcal{L}_{,X}$, which together completely specify the inflationary dynamics. In this paper, we fix the gauge by setting [29]

$$\mathcal{L}_{,X} = c_s^{-1}, \quad (12)$$

which leads to the following hierarchies of flow parameters [30],

$$\begin{aligned}
\epsilon(\phi) &\equiv \frac{2M_{\rm Pl}^2}{\gamma(\phi)}\left(\frac{H'(\phi)}{H(\phi)}\right)^2,\\
\eta(\phi) &\equiv \frac{2M_{\rm Pl}^2}{\gamma(\phi)}\frac{H''(\phi)}{H(\phi)},\\
&\vdots\\
{}^{\ell}\lambda(\phi) &\equiv \left(\frac{2M_{\rm Pl}^2}{\gamma(\phi)}\right)^{\ell}\left(\frac{H'(\phi)}{H(\phi)}\right)^{\ell-1}\frac{1}{H(\phi)}\frac{d^{\ell+1}H(\phi)}{d\phi^{\ell+1}},\\
s(\phi) &\equiv \frac{2M_{\rm Pl}^2}{\gamma(\phi)}\frac{H'(\phi)}{H(\phi)}\frac{\gamma'(\phi)}{\gamma(\phi)},\\
\rho(\phi) &\equiv \frac{2M_{\rm Pl}^2}{\gamma(\phi)}\frac{\gamma''(\phi)}{\gamma(\phi)},\\
&\vdots\\
{}^{\ell}\alpha(\phi) &\equiv \left(\frac{2M_{\rm Pl}^2}{\gamma(\phi)}\right)^{\ell}\left(\frac{H'(\phi)}{H(\phi)}\right)^{\ell-1}\frac{1}{\gamma(\phi)}\frac{d^{\ell+1}\gamma(\phi)}{d\phi^{\ell+1}}, \quad (13)
\end{aligned}$$

where $\ell = 2, \cdots, \infty$ is an integer index. For the remainder of this paper, we will refer to the parameters ${}^{\ell}\lambda(\phi)$ and ${}^{\ell}\alpha(\phi)$ as the ℓ-th components of the *H-tower* and *γ-tower* respectively. In the case where $\gamma = 1$, the γ-tower vanishes and the above hierarchy reduces to the flow hierarchy of a canonical scalar field [31, 32].

We next Taylor expand the Hubble parameter about $\phi_0 = 0$,

$$H(\phi) = H_0\left[1 + \sum_{\ell=1}^{\mathcal{M}+1} A_\ell\left(\frac{\phi}{M_{\rm Pl}}\right)^{\ell}\right], \quad (14)$$

and the inverse speed of sound

$$\gamma(\phi) = \gamma_0\left[1 + \sum_{\ell=1}^{\mathcal{N}+1} B_\ell\left(\frac{\phi}{M_{\rm Pl}}\right)^{\ell}\right], \quad (15)$$

where the expansions are truncated at orders $\mathcal{M}+1$ and $\mathcal{N}+1$, respectively,

$$\begin{aligned}
\frac{d^{\ell}H(\phi)}{d\phi^{\ell}} &= 0 \quad \text{for} \quad \ell \geq \mathcal{M}+2,\\
\frac{d^{\ell}\gamma(\phi)}{d\phi^{\ell}} &= 0 \quad \text{for} \quad \ell \geq \mathcal{N}+2. \quad (16)
\end{aligned}$$

In fact, this truncation is equivalent to simply setting ${}^{\mathcal{M}+1}\lambda = {}^{\mathcal{N}+1}\alpha = 0$ in the flow hierarchy, for reasons that will become clear in Section IV.

The coefficients A_ℓ and B_ℓ are given by [30]

$$\begin{aligned}
A_1 &= \sqrt{\epsilon_0\gamma_0/2},\\
A_{\ell+1} &= \frac{(\gamma_0/2)^{\ell}}{(\ell+1)!A_1^{\ell-1}}\left({}^{\ell}\lambda_0\right), \quad (17)
\end{aligned}$$

and

$$\begin{aligned}
B_1 &= \frac{s_0\gamma_0/2}{A_1},\\
B_{\ell+1} &= \frac{(\gamma_0/2)^{\ell}}{(\ell+1)!A_1^{\ell-1}}\left({}^{\ell}\alpha_0\right). \quad (18)
\end{aligned}$$

While this particular parameterization restricts $H(\phi)$ and $\gamma(\phi)$ to be polynomials, these functions can be made more general by truncating Eq. (13) at arbitrarily high order. The values of the flow parameters at some $\phi = \phi_0$ fully define the functions $H(\phi)$ and $\gamma(\phi)$, completely determining the theory in the gauge $\mathcal{L}_{,X} = c_s^{-1}$.

B. DBI Inflation

In what follows, we will study DBI inflation as a prototype non-canonical model. The only model-dependent results in this paper are those relating non-Gaussianities to the sound speed, c_s. However, as we will discuss further, the qualitative nature of our results should apply generically to non-canonical models. DBI inflation refers to models arising from the action of D-branes in flux compactifications of type-IIB string theory [18, 33, 34]. Typically, the inflaton field parameterizes the separation of a probe D3-brane and a stack of $\overline{\rm D3}$-branes in a warped throat geometry. This geometry is defined by the line element [35],

$$ds_{10}^2 = h^{-1/2}(y)g_{\mu\nu}dx^{\mu}dx^{\nu} + h^{1/2}(y)\left(d\rho^2 + \rho^2 ds_{X_5}^2\right), \quad (19)$$

where the internal space is a cone over the five-manifold X_5. The inflaton field is proportional to the throat coordinate ρ by $\phi = \sqrt{T_3}\rho$, where T_3 is the tension on the D3-brane. The Lagrangian for the inflaton is then of the form [34]

$$\mathcal{L} = -f^{-1}(\phi)\sqrt{1 + f(\phi)g^{\mu\nu}\partial_{\mu}\phi\partial_{\nu}\phi} + f^{-1}(\phi) - V(\phi), \quad (20)$$

where $V(\phi)$ is the scalar field potential and the function $f(\phi)$ is related to the warp factor $h(\phi)$ by

$$f(\phi) = \frac{1}{T_3 h^4(\phi)}. \tag{21}$$

The γ-factor defined by

$$\gamma = \frac{1}{\sqrt{1 - f(\phi)\dot{\phi}^2}}, \tag{22}$$

enforces a speed limit on the moduli space, arising from causality constraints on the motion of the probe brane in the throat. This phenomenon mitigates the η-problem associated with potentials derived from supergravity, allowing for otherwise too steep potentials to successfully drive inflation.

The equations of motion are easily obtained from our previous results. The Friedmann equation (6) becomes [36],

$$3M_{\rm Pl}^2 H^2(\phi) - V(\phi) = \frac{\gamma(\phi) - 1}{f(\phi)}, \tag{23}$$

which gives

$$\dot{\phi} = -\frac{2M_{\rm Pl}^2}{\gamma(\phi)} H'(\phi). \tag{24}$$

Equation (22) then becomes,

$$\gamma = \sqrt{1 + 4M_{\rm Pl}^4 f(\phi) \left[H'(\phi)\right]^2}. \tag{25}$$

These results lead to the Hamilton-Jacobi equation,

$$V(\phi) = 3M_{\rm Pl}^2 H^2(\phi) - 4M_{\rm Pl}^4 \frac{H'^2(\phi)}{\gamma(\phi) + 1}, \tag{26}$$

which can be used to reconstruct the scalar potential given the functions $H(\phi)$ and $\gamma(\phi)$. The warp factor of the geometry can also be reconstructed from these two functions via Eq. (25). The Taylor expansions Eq. (14) and (15) can then be used to obtain exact expressions for $V(\phi_0)$ and its derivatives. In this work, we will only require expressions for the first two derivatives of $V(\phi)$. After some tedious but straightforward algebra we obtain,

$$\begin{aligned} V(\phi_0) &= M_{\rm Pl}^2 H^2 \left(3 - 2\epsilon\Gamma\right), \\ V'(\phi_0) &= M_{\rm Pl} H^2 \sqrt{2\epsilon\gamma} \left(3 - 2\eta\Gamma + s\Gamma^2\right), \\ V''(\phi_0) &= H^2\gamma \left[3\left(\epsilon + \eta\right) - 2\left(\eta^2 + \xi\right)\Gamma \right. \\ &\quad \left. + 2s\left(2\eta - s\Gamma\right)\Gamma^2 + \epsilon\rho\Gamma^2\right], \end{aligned} \tag{27}$$

where

$$\Gamma = \frac{\gamma}{\gamma + 1}. \tag{28}$$

In the next section, we utilize these results to obtain observational constrains on the inflaton potential from a synthetic data-set.

III. PROJECTIONS FOR PLANCK: MCMC ANALYSIS

In this section, we constrain the inflaton potential in the hypothetical case that Planck detects tensors, with $r = 0.1$, but fails to positively detect any non-Gaussianities, implying $|f_{NL}| \lesssim 5$. Such an observation would certainly be consistent with canonical inflation, for which $c_s = 1$. However, it would also be consistent with a host of more exotic, non-canonical models, such as k-inflation and DBI. The speed of sound varies in such models and gives rise to detectable non-Gaussianities if $c_s \ll 1$. From Eq. (10), we have for the case of DBI inflation,

$$f_{NL} = \frac{35}{108}\left(\frac{1}{c_s^2} - 1\right). \tag{29}$$

However, even for non-detectable values of f_{NL}, we see that the sound speed can vary considerably, $0.25 \lesssim c_s \leq 1$. In non-canonical models, there is another way to measure c_s, however, independent of the strength of non-Gaussianities. These models predict a modified consistency relation [28],

$$r = -8 c_s n_t, \tag{30}$$

where n_t is the tensor spectral index. The downside is that this relation will be very difficult to reliably measure any time in the near future. Even a direct detection of primordial gravity waves from proposed BBO [37] or DECIGO [38] will only measure this relation to within an accuracy of 50% [39]. The uncertainty in the value of c_s thus remains. How might this affect our ability to reconstruct $V(\phi)$?

In models with a variable speed of sound, the scalar and tensor amplitudes are given during slow roll by,

$$P_{\mathcal{R}}(k) = \frac{1}{8\pi^2 M_{\rm Pl}^2} \left.\frac{H^2}{c_s \epsilon}\right|_{k c_s = aH}, \tag{31}$$

and

$$P_h(k) = \frac{2}{\pi^2} \left.\frac{H^2}{M_{\rm Pl}^2}\right|_{k = aH}, \tag{32}$$

where we note that scalar perturbations freeze out upon exiting the sound horizon, whereas tensor perturbations do so upon exiting the Hubble radius. Often in the literature, the tensor/scalar ratio is written $r = 16 c_s \epsilon$, obtained from Eqs. (31) and (32) by neglecting this difference in freeze out times (assuming that H is constant). This is not strictly correct. While this difference enters at 2^{nd}-order in slow roll, it can be important if c_s is small[1].

[1] The limited accuracy of this expression was recently noted in Ref. [29], where numerical spectrum calculations reveal discrepancies of up to 50%.

The evolution of H is determined by

$$\frac{dH}{dN} = \epsilon H, \tag{33}$$

where N is defined as the number of e-folds before the end of inflation. From the horizon crossing conditions we form the ratio,

$$\frac{H_t}{H_s} = \frac{1}{c_s}\frac{a_s}{a_t}, \tag{34}$$

where the subscripts t and s indicate that these values are measured when the tensor and scalar perturbations exit their respective horizons. If we suppose that ϵ is constant between these crossing times (an excellent assumption during slow roll), this ratio becomes

$$e^{\epsilon(N_t - N_s)} = c_s^{-1} e^{N_t - N_s}, \tag{35}$$

with the result that the change in the number of e-folds between the time that a certain scalar k-mode exits the sound horizon and the time the corresponding tensor mode exits the event horizon is given by,

$$N_s - N_t = \frac{\ln c_s}{\epsilon - 1}. \tag{36}$$

The tensor/scalar ratio is then[2]

$$\begin{aligned} r = \frac{P_h(k)}{P_{\mathcal{R}}(k)} = 16\epsilon c_s \left(\frac{H_t}{H_s}\right)^2 &= 16\epsilon c_s e^{2\epsilon(N_t - N_s)} \\ &= 16\epsilon c_s^{\frac{1+\epsilon}{1-\epsilon}}. \end{aligned} \tag{37}$$

The scalar spectral index of the power spectrum is also affected by the variable speed of sound. At lowest-order in slow roll,

$$n_s = 1 - 4\epsilon + 2\eta - 2s, \tag{38}$$

where η and s are defined in Eq. (13). The tensor spectral index is written

$$n_t = -2\epsilon, \tag{39}$$

which leads to the modified consistency relation at lowest order, $r = -8 c_s n_t$.

We are now in a position to determine what effect a non-detection of f_{NL} has on reconstruction efforts. From our results in the previous section Eq. (27) we can link $V(\phi)$ to the observables $P_{\mathcal{R}}$, r, n_s, and f_{NL}. In this section we work to lowest-order in slow roll and assume that c_s is constant. We neglect any running of the spectra and thus work to reconstruct $V(\phi_0)$ and its first two derivatives. In terms of observables these are written,

$$\begin{aligned} \frac{V(\phi_0)}{M_{\rm Pl}^4} &= \frac{\pi^2}{2} P_{\mathcal{R}} r \left[3 - \frac{\gamma^2 r}{8(\gamma+1)}\right], \\ \frac{V'(\phi_0)}{M_{\rm Pl}^3} &= \frac{\sqrt{2}\pi^2}{16} P_{\mathcal{R}} r^{3/2} \gamma \left[6 - \frac{\gamma}{2}\frac{(4n_s + r\gamma - 4)}{\gamma+1}\right], \\ \frac{V''(\phi_0)}{M_{\rm Pl}^2} &= \frac{\pi^2}{4} P_{\mathcal{R}} r\gamma \left[3\left(n_s - 1 + \frac{3}{8} r\gamma\right)\right. \\ &\quad \left. - \frac{\gamma}{2}\frac{(4n_s + r\gamma - 4)^2}{\gamma+1}\right], \end{aligned} \tag{40}$$

where the observables are to be measured at the scale corresponding to ϕ_0. We have used γ rather than the observable f_{NL} in these expressions for simplicity. It is now clear how any uncertainty in γ will translate into uncertainties in the potential. The height of the potential, $V(\phi_0)$, will be least affected, however, $V'(\phi_0)$ and $V''(\phi_0)$ will be more strongly so because they are directly proportional to γ.

In order to rigorously analyze the effects of an unresolved speed of sound, we constrain $V(\phi_0)$ and its first two derivatives using Markov Chain Monte Carlo (MCMC) and a simulated, Planck-precision CMB dataset. We use the publicly available `CosmoMC`[3] [41] package to explore the inflationary parameter space. We constrain $V(\phi)$ arising from non-canonical models by allowing c_s to vary in the analysis, and compare this case to constraints obtained on $V(\phi)$ arising from canonical inflation, obtained by fixing $c_s = 1$.

MCMC techniques [42–45] sample the likelihood surface of model parameters, $\mathcal{L}(\mathbf{d}|\boldsymbol{\theta})$, where $\mathbf{d}$ represents the n-dimensional data and $\boldsymbol{\theta}$ the n-dimensional parameter vector. The likelihood function relates any prior knowledge of the parameter values, $\pi(\boldsymbol{\theta})$, to the posterior probability distribution via Bayes' theorem,

$$p(\boldsymbol{\theta}|\mathbf{d}) = \frac{\mathcal{L}(\mathbf{d}|\boldsymbol{\theta})\pi(\boldsymbol{\theta})}{P(\mathbf{d})} = \frac{\mathcal{L}(\mathbf{d}|\boldsymbol{\theta})\pi(\boldsymbol{\theta})}{\int \mathcal{L}(\mathbf{d}|\boldsymbol{\theta})\pi(\boldsymbol{\theta}) d\boldsymbol{\theta}}. \tag{41}$$

The posterior probability distribution function (PDF) of a single parameter θ_i can then be obtained by marginalizing $p(\boldsymbol{\theta}|\mathbf{d})$ over the remaining parameters,

$$p(\theta_i|\mathbf{d}) = \int p(\boldsymbol{\theta}|\mathbf{d}) d\theta_1 \cdots d\theta_{i-1} d\theta_{i+1} \cdots d\theta_{n-1}. \tag{42}$$

In this study, we only constrain the inflationary parameters ($V(\phi)$, $V'(\phi)$, $V''(\phi)$, and c_s), fixing the late-time parameters at the values: baryon and CDM densities, $\Omega_b h^2 = 0.022$ and $\Omega_c h^2 = 0.104$, the angular diameter distance at decoupling, $\theta_s = 1.04$, and the optical depth to reionization, $\tau = 0.093$. Degeneracies amongst the late-time parameters and the power spectrum do exist, in particular, n_s is still moderately degenerate with $\Omega_b h^2$. However, our goal in this study is to compare the constraints obtained on $V(\phi)$ when c_s is allowed to vary and when it is held constant at $c_s = 1$. In both of these cases the spectrum is completely described by the parameters

[2] See Ref. [40] for an alternative derivation.

[3] http://cosmologist.info/cosmomc/

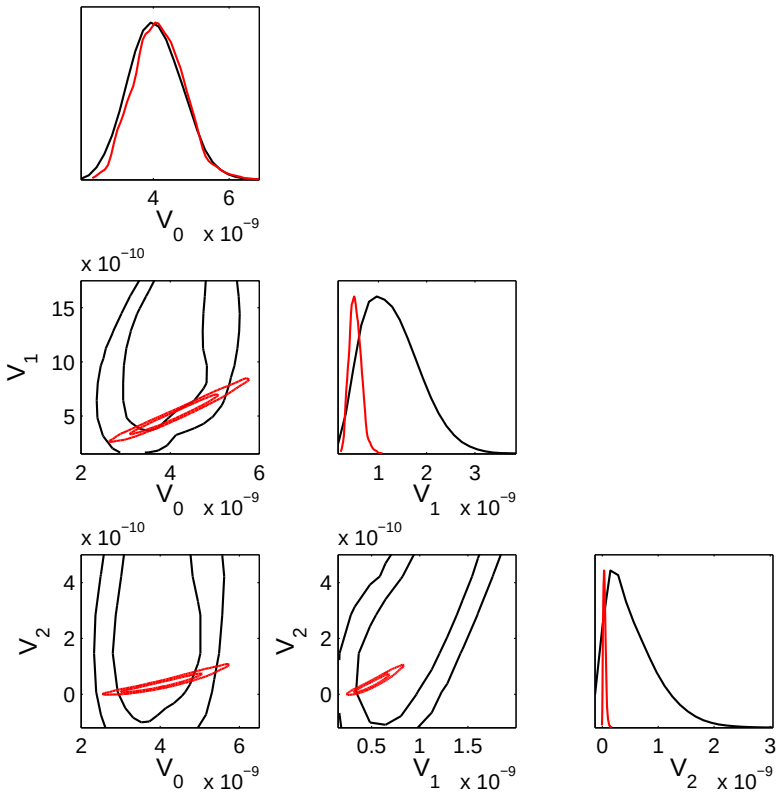

FIG. 1: Marginalized 1- and 2-D PDF's of the potential parameters, $V_0 = V(\phi_0)$, $V_1 = V'(\phi_0)$, and $V_2 = V''(\phi_0)$ in units of $M_{\rm Pl}$. The small red contours correspond to 1- and 2-σ errors in canonical inflation, in which c_s is held fixed at 1. The substantially larger black contours correspond to non-canonical inflation in which c_s is allowed to vary in the chains between 0.25 and 1.

$P_{\mathcal{R}}$, r, n_s, and n_t, and so the introduction of c_s as a free parameter will not introduce new degeneracies.

Our Planck-precision simulation comprises temperature, E- and B-mode polarization data out to $\ell = 2500$ with a sky coverage of 65%. For simplicity, we consider a single-channel experiment in which the full width at half maximum of the Gaussian beam, $\theta_{\rm fwhm} = 7'$, and the root mean square of the pixel noise, $\sigma_T^2 = \sigma_P^2/2 = 30.25\mu{\rm K}^2$. As a fiducial model we choose a power-law spectrum with $P_{\mathcal{R}}(k = 0.002h\,{\rm Mpc}^{-1}) = 2.3 \times 10^{-9}$, $n_s = 0.97$, and $r = 0.1$. We assume the inflationary consistency relation for the tensor spectral index, $n_t = -\gamma r/8$. We impose the prior $c_s \in [0.25, 1]$, consistent with undetectable non-Gaussianities. We assume purely adiabatic initial perturbations and spatial flatness, and adopt a top-hat prior on the age of the universe: $10 < t_0 < 20\,{\rm Gyr}$. We utilize the Metropolis-Hastings sampling algorithm and measure convergence across 8 chains with the Gelman-Rubin R statistic.

We present our results in Figure 1 and Table 1. Both best-fit reconstructions fit the data equally well: $-2\ln\mathcal{L} = 7931.29$ for the canonical and $-2\ln\mathcal{L} = 7931.16$ for the non-canonical reconstruction. The two models are thus statistically degenerate. The red contours in the figure correspond to 1- and 2-σ errors for canonical inflation, for which c_s is held fixed at 1. The black contours correspond to non-canonical inflation in which c_s is allowed to vary in the chains between 0.25 and 1. Indeed, the constraints on $V(\phi)$ worsen significantly if c_s is included in the reconstruction. This is a significant impediment to the program of potential reconstruction: if we allow for the possibility of an arbitrary speed of sound, reconstruction of the potential is severely degraded in the absence of a measurement of the amplitude of non-Gaussianities. Table I indicates that the marginalized errors on V_1 and V_2 increase by an order of magnitude in going from canonical to non-canonical inflation. While we have used Eq. (29) specific to DBI inflation, the fact that a failure to resolve non-Gaussianities precludes a unique inversion of the power spectrum is a general result. We therefore expect this problem to persist in general non-canonical models, however, the degree of the effect is model dependent.

It is interesting to note how well constrained the canonical model is. In particular, the absolute errors on V'' are *smaller* than those obtained on V'. The dominant term in the error on V'' is proportional to $3\pi^2\delta r P_{\mathcal{R}}(n_s - 1)/2$, whereas the dominant term in the error on V' is $\delta V' \sim P_{\mathcal{R}}(r + \delta r)^{3/2} - V'$. For Planck-precision errors on r, the two terms in $\delta V'$ are of the same order, and so $\mathcal{O}(\delta V') \sim \mathcal{O}(V')$. For the values of our fiducial model,

Model	$V_0 \times 10^9 M_{\rm Pl}^{-4}$	$V_1 \times 10^{10} M_{\rm Pl}^{-3}$	$V_2 \times 10^{11} M_{\rm Pl}^{-2}$
canonical	$3.7^{+1.9}_{-0.7}$	$4.3^{+3.7}_{-1.2}$	$2.5^{+7.2}_{-1.8}$
non-canonical	$3.6^{+1.9}_{-0.9}$	16^{+10}_{-12}	91^{+80}_{-90}

TABLE I: Marginalized 2-σ errors on the potential parameters of each model.

$(r+\delta r)^{3/2} \approx \delta r$, and so roughly we have

$$\delta V'' \approx \frac{3}{2}\pi^2 (n_s - 1)\delta V' \sim \mathcal{O}(10^{-1})\delta V'. \qquad (43)$$

In Figure 2 we plot the reconstructed best fit potentials for each model. As indicated by the error contours and by this figure, the speed of sound has the effect of rendering steep potentials viable. This is precisely the novel aspect that initially popularized DBI inflation, but as we see here, is a bane to reconstruction efforts if f_{NL} goes undetected. However, the detection of tensor modes still reliably determines the energy scale of inflation. For $r = 0.1$, the uncertainty introduced by c_s is only around 1%. The energy scale reconstructed from the observables is measured at $\phi = 0$ in Figure 2.

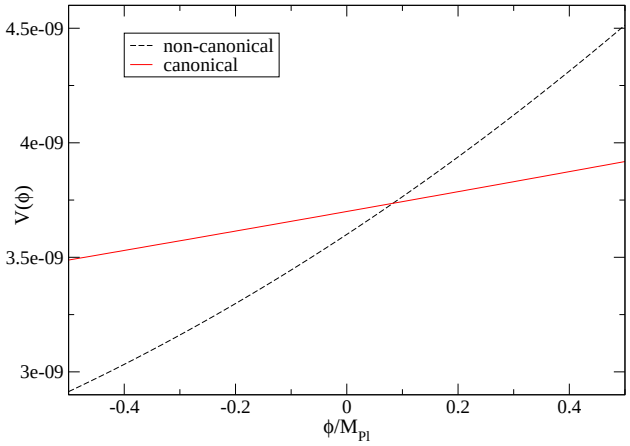

FIG. 2: Potentials reconstructed from the best-fit parameters of Table 1. Note the increased steepness of the non-canonical potential (black dashed) relative to the canonical potential (red solid).

IV. PROJECTIONS FOR PLANCK: FLOW ANALYSIS

While the MCMC method utilized in the last section is a rigorous Bayesian analysis of the parameter space, it performs poorly if too many free parameters are included in the fit. This is especially true if some of these parameters are degenerate or poorly constrained by the data. It is therefore not feasible to go much beyond the lowest-order analysis ($c_s = $ const.) conducted in the previous section. In this section, we use the flow formalism [32, 46] as a method for reconstructing inflationary potentials compatible with future observations. While not statistically rigorous, the flow method is well suited to studying the inflationary parameter space to arbitrarily high order in slow roll. It is also capable of reconstructing models with a varying sound speed. In this section, we utilize the flow formalism in order to study parameter constraints in the event that a tensor signal is detected in the future, but non-Gaussianities are not. This is the same scenario considered in the last section, but here we examine the effects of allowing a time-varying speed of sound. We conclude this section by considering the case of a positive detection of non-Gaussianities.

The flow formalism is based on the property of the flow parameters defined in Eq. (13), that their evolution in terms of the number of e-folds N can be described by a set of first order differential equations. Taking successive derivatives of the flow parameters with respect to N, we obtain the *flow equations*

$$\begin{aligned}
\epsilon &= \frac{1}{H}\frac{dH}{dN}, \\
\frac{d\epsilon}{dN} &= \epsilon\,(2\eta - 2\epsilon - s)\,, \\
\frac{d\eta}{dN} &= -\eta\,(\epsilon + s) + {}^2\lambda, \\
&\vdots \\
\frac{d^\ell \lambda}{dN} &= -{}^\ell\lambda\,[\ell\,(s+\epsilon) - (\ell-1)\,\eta] + {}^{\ell+1}\lambda, \\
s &= \frac{1}{\gamma}\frac{d\gamma}{dN}, \\
\frac{ds}{dN} &= -s\,(2s + \epsilon - \eta) + \epsilon\rho, \\
\frac{d\rho}{dN} &= -2\rho s + {}^2\alpha, \\
&\vdots \\
\frac{d^\ell \alpha}{dN} &= -{}^\ell\alpha\,[(\ell+1)\,s + (\ell-1)\,(\epsilon - \eta)] + {}^{\ell+1}\alpha, \qquad (44)
\end{aligned}$$

where the derivative of a flow parameter is related to terms of higher-order in the flow hierarchy. In practice, the flow equations are truncated at some finite order $\mathcal{M}$ and $\mathcal{N}$ by requiring that ${}^\ell\lambda = {}^\ell\alpha = 0$ for all $\ell \geq \mathcal{M}+1$ and $\mathcal{N}+1$, respectively, at the initial time. By Eq. (44), these remain zero for all time with the result that the trajectory so obtained is an *exact* solution to the inflationary equations of motion.

This truncated system of differential equations can be solved numerically by specifying the set of initial conditions for the flow parameters $\left[H, \epsilon, \ldots, {}^{\mathcal{M}}\lambda; \gamma, s, \ldots, {}^{\mathcal{N}}\alpha\right]\big|_{N_0}$ at some time N_0. The solution will then be a particular inflationary path $\left[H(N), \epsilon(N), \ldots, {}^{\mathcal{M}}\lambda(N); \gamma(N), s(N), \ldots, {}^{\mathcal{N}}\alpha(N)\right]$ in the $(\mathcal{M}+\mathcal{N})$-dimensional parameter space. In fact, the expansions Eqs. (14) and (15) yield exact analytic solutions of the flow equations, where the expansions

can be taken about any point along the inflationary trajectory [47]. In this paper, we truncate the flow hierarchy to second order in the H-tower, and to first order in the γ-tower so that

$$ {}^{\ell}\lambda = {}^{\ell'}\alpha = 0, \tag{45}$$

for all $\ell > 2$ and $\ell' > 1$. The resulting solution to the flow equations will then be a specific path $[\epsilon(N), \eta(N), \xi(N), s(N), \rho(N)]$ in the 5-dimensional parameter space. The inclusion of s and ρ allows us to generate models with a varying speed of sound. We solve the flow equations from the time the quadrupole leaves the horizon at $N_{\rm quad}$ up until the smallest scale modes detectable in the CMB are generated, a period typically spanning 10 e-folds. We restrict this analysis to models that do not violate causality, $c_s \leq 1$. We then calculate the observables from the values of the flow parameters at $N = N_{\rm quad}$,

$$\begin{aligned} n_s &= 1 - 4\epsilon + 2\eta - 2s - 2(1+C)\epsilon^2 - (3+C)s^2 \\ &\quad -\frac{1}{2}(3-5C)\epsilon\eta - \frac{1}{2}(11+3C)\epsilon s + (1+C)\eta s \\ &\quad +\frac{1}{2}(1+C)\epsilon\rho + \frac{1}{2}(3-C)({}^2\lambda), \\ r &= 16 c_s \epsilon \left[1 + \frac{1}{2}(\epsilon-\eta)(C-3) + \frac{s}{2}(C+1)\right], \\ \alpha &= -\left(\frac{1}{1-\epsilon-s}\right)\frac{dn_s}{dN}, \\ f_{NL} &= \frac{35}{108}\left(\frac{1}{c_s^2} - 1\right), \end{aligned} \tag{46}$$

where

$$ C = 4(\ln 2 + \gamma) - 5, \tag{47}$$

and $\gamma \simeq 0.577$ is the Euler-Mascheroni constant, which should not be confused with the inverse sound speed Eq. (22).

A. Detection of r and no detection of f_{NL}

We are interested in collecting models compatible with the simulated data of Section III,

$$\begin{aligned} n_s &= 0.97 \pm 0.0036, \\ r &= 0.1 \pm 0.05, \\ \alpha &= 0.0 \pm 0.005, \\ 10^9 P_{\mathcal{R}} &= 2.3 \pm 0.102, \end{aligned} \tag{48}$$

where the errors are 1-σ projections for Planck, quoted at $k = 0.002\,h{\rm Mpc}^{-1}$. The observables calculated at the quadrupole by the flow method are easily extrapolated to $k = 0.002\,h{\rm Mpc}^{-1}$ because the spectra are power-laws. In order to efficiently generate models with power-law spectra, we truncate the H-tower at ξ^2. The inclusion of higher-order terms not only affects the running, but may even make a non-negligible contribution to higher-order k-dependencies in the power spectrum. Since we do not have analytic expressions[4] for these higher-order terms, we can not be sure that they are under control. By working only up to order ξ^2, and by ensuring that the running is small, we can be certain that all higher-order terms will likewise be small, since they are at least of order ξ^4. Most viable models at this order naturally have small running anyway, since large negative running at order ξ^2 typically leads to an insufficient amount of inflation [48].

We now use this methodology to stochastically generate models of inflation consistent with the constraints Eq. (48). We are interested in models which fail to generate observable non-Gaussianities, corresponding to a speed of sound in the range $c_s \in [0.25, 1]$ (c.f. Eq. (29)). We first seek to reconstruct models with a constant speed of sound in order to make contact with the results of section 3, and so the γ-tower is simply replaced by $c_s = $ const. After obtaining results for constant speed of sound, we perform the analysis for a variable speed of sound by allowing s and ρ to vary.

We present our results in Figure 3. We plot the values of V_0, $V_1 = V_0'$, and $V_2 = V_0''$ for canonical inflation, where $c_s = 1$ (red squares), DBI inflation with constant speed of sound (black circles), and DBI inflation with varying speed of sound (green crosses) using Eqs. (27). It can easily be seen that, even though we can not make any rigorous statistical arguments using the flow formalism, we successfully reproduce the results found in the previous section using MCMC techniques. The most striking consequence of a variable speed of sound is that a large region of parameter space for which $V_0'' < 0$ opens up. To understand this, note from Eq. (27) that the sign of V'' to lowest-order is determined by the sign and magnitude of η. In the case of constant sound speed, the value of η is tightly constrained by the spectral index, $n_s = 1 - 4\epsilon + 2\eta$. However, if c_s is allowed to vary, then the spectral index becomes

$$ n_s = 1 - 4\epsilon + 2\eta - 2s, \tag{49}$$

to lowest-order. For a given value of n_s, η can be taken more negative by suitably adjusting s. From Eq. (27), this allows a wide range of parameter space for which $V_0'' < 0$ to be brought into agreement with the data. Physically, the steepening of the potential that results from tuning η is mitigated by the increased warping of the geometry, which is related to the value of the flow parameter s.

B. Detection of f_{NL}

In this section, we are interested in models which are characterized by detectable non-Gaussianity for both ob-

[4] This issue is avoided by calculating the power spectra numerically, as done in [29].

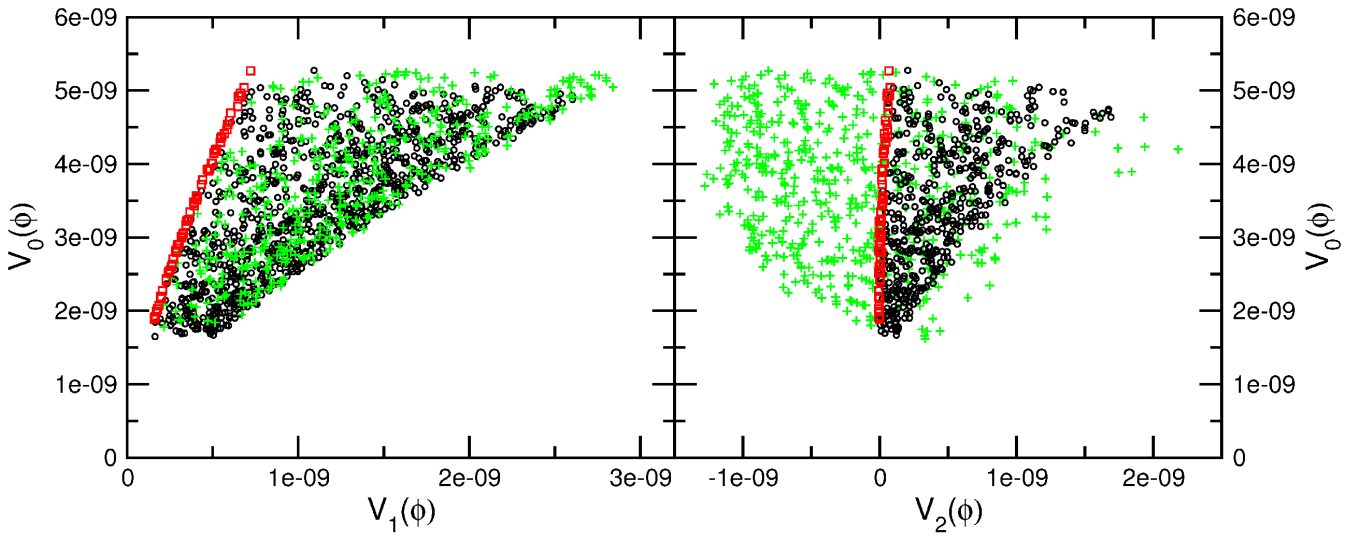

FIG. 3: Results of the flow analysis for the case of detection of r, with $r = 0.1 \pm 0.05$ but no f_{NL} ($f_{NL} < 5$). Red squares are canonical models, black circles DBI inflation with constant speed of sound, and green crosses DBI models with variable speed of sound. The case of variable speed of sound opens up the parameter space for which $V_0'' < 0$.

servational outcomes of gravity waves. We start by considering the case in which future data fails to detect any gravity waves, but *does* successfully detect evidence for non-Gaussian fluctuations. While it is well known that a failure to detect tensors precludes a lower bound on the energy scale of inflation, it might be hoped that a positive detection of non-Gaussianities yields improved constraints relative to the worst case scenario in which neither is detected. The simulated data used thus far in the study does not apply to this case. However, taking the scalar perturbations to be the same, we collect models that satisfy Eq. (48) for n_s, $P_{\mathcal{R}}$, and α. In order for Planck to fail to detect tensors, we suppose that the null hypothesis ($r = 0$) is verified for $r \leq 0.05$.

We show the results of the flow analysis in Figure 4. We consider detection of non-Gaussianities at two different levels: $f_{NL} = 10$ and $f_{NL} = 40$, with 1-σ errors $\Delta f_{NL} = \pm 5$. By failing to detect r, we only succeed in placing an upper bound on the values of V_0 and V_0'. However, a determination of γ tightly correlates V_0 with both V_0' and V_0''. From Eq. (41) we have that

$$V \sim \left(\frac{P_{\mathcal{R}}(k)}{\gamma^2}\right)^{1/3} V'^{2/3}, \tag{50}$$

and

$$V \sim \frac{P_{\mathcal{R}}(k)}{\gamma}\left[-1 + \sqrt{\frac{4V''}{3P_{\mathcal{R}}(k)}\frac{1}{n_s - 1}}\right]. \tag{51}$$

The uncertainty in r only allows us to constrain the above relationships between the potential parameters. These relations give the distinctive band structure seen in Figure 4. The effect of the detection of non-Gaussianities on these constraints is two-fold: the value of γ controls the 'slope' of the bands, and, as we show next, the relative error between V-V' and V-V''.

The contribution of the error Δf_{NL} to V' and V'' depends on the absolute value of f_{NL}. Since this is the dominant source of error, a determination of f_{NL} can thus improve constraints. To see this, consider the case of V'. Including only the contribution of f_{NL} to the error on V', we have

$$\delta V' \propto \left(\sqrt{f_{NL} + \Delta f_{NL}} - \sqrt{f_{NL} - \Delta f_{NL}}\right)\delta V, \tag{52}$$

and expanding the square roots for small Δf_{NL} relative to f_{NL} gives

$$\delta V' \propto \frac{\Delta f_{NL}}{\sqrt{f_{NL}}}\delta V. \tag{53}$$

Thus, a determination of f_{NL} correlates the errors in V and V', and similarly for V and V'' (c.f. Figure 4). Additionally, the larger the value of f_{NL}, the smaller this relative error between the potential coefficients. Therefore, while a detection of r allows us to constrain the absolute scale of the inflationary potential and its derivatives, a detection of f_{NL} gives us information about the *relative* values of these parameters, as well as being a smoking gun for exotic physics.

Finally, we consider the case where *both* r and f_{NL} are detected. We collect models that satisfy Eq. (48), and produce detectable non-Gaussianities at the level of $f_{NL} = 10$ with 1-σ errors $\Delta f_{NL} = \pm 5$. We present the results of the flow analysis in Figure 5, where it can be seen that we again obtain the band-shaped distributions for the potential parameters. Following the reasoning of the previous sections, we see that the detection of r places bounds on the potential parametes, where the de-

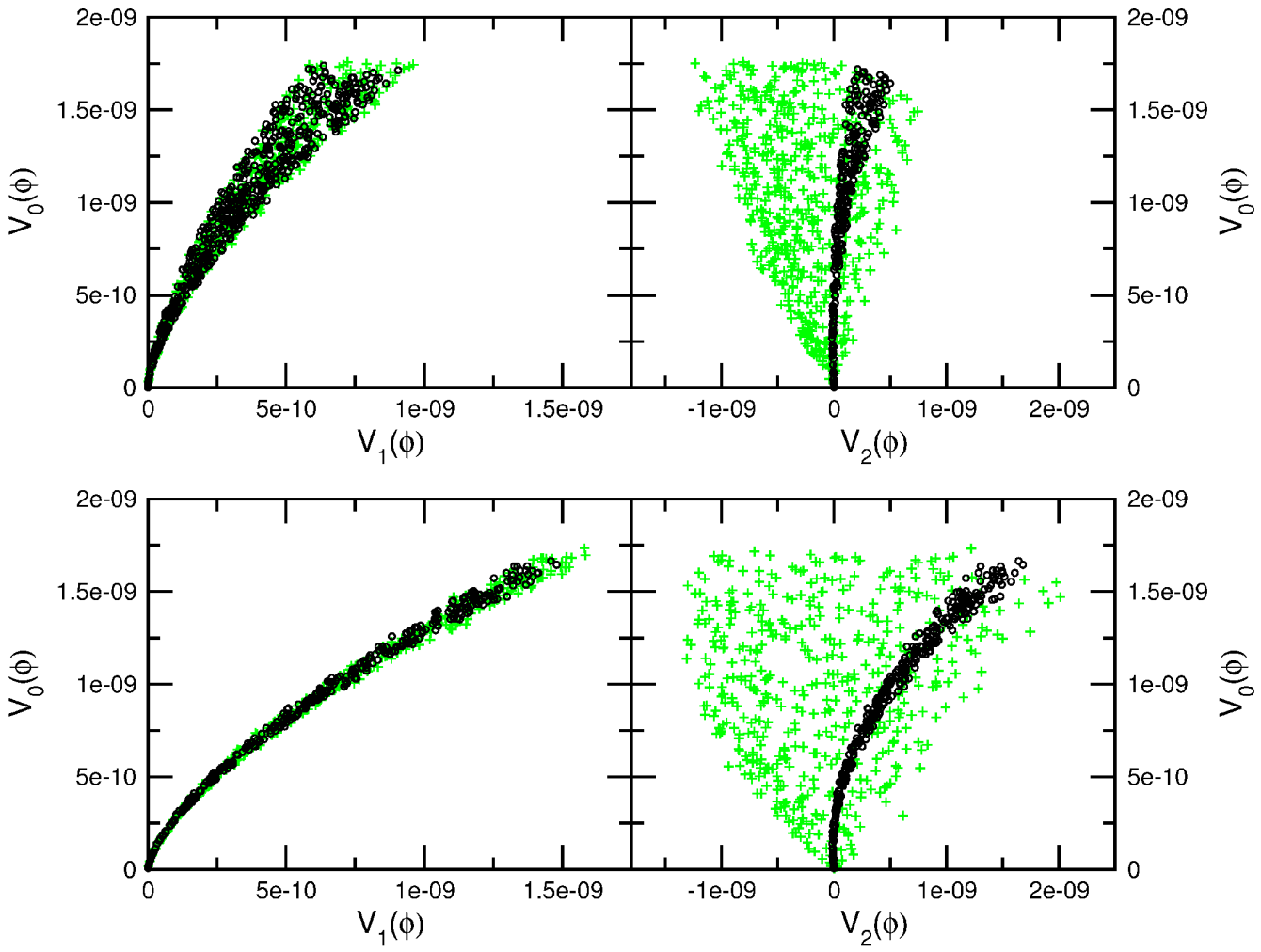

FIG. 4: Results of the flow analysis for the case of detection of f_{NL} but no r ($r \leq 0.05$). The top figure corresponds to models with $f_{NL} = 10 \pm 5$, and the bottom one to models with $f_{NL} = 40 \pm 5$. Black circles are DBI models with constant speed of sound, and green crosses DBI models with variable speed of sound.

tection of non-Gaussianities determines the relative error amongst them.

V. CONCLUSIONS

We have considered potential reconstruction forecasts for the upcoming Planck Surveyor CMB mission in the context of non-canonical inflation. We have focused on the following observational outcomes: a detection of a tensor signal and a null detection of non-Gaussianities, a null detection of tensors and a positive detection of non-Gaussianities, and a positive detection of both tensors and non-Gaussianities. To explore the first case, we perform a Markov Chain Monte Carlo analysis on a simulated Planck-precision data-set. We obtain constraints on the potential parameters V_0, V_0', and V_0'', and the sound speed c_s. A null detection of non-Gaussianities at Planck resolution corresponds to $|f_{NL}| \lesssim 5$, with the result that c_s is only constrained to lie within the range $[0.25, 1]$ for the case of DBI inflation. Since c_s also affects the form of the power spectrum, a failure to constrain it precludes us from inverting our spectrum observation to obtain the inflaton potential. The errors on V_0' and V_0'' increase by an order of magnitude relative to constraints obtained on canonical inflation.

We next used the flow formalism to investigate the effect of allowing the speed of sound to vary over the course of inflation. This requires the introduction of terms governing its evolution. Unlike MCMC methods, the flow formalism is well suited to studying reconstructions to high-order. The strongest effect of a variable speed of sound is a much increased error on the second derivative of $V(\phi)$. A variable speed is generic to models such as DBI inflation. The worsening of the constraint on V_0'' results from the fact that there is additional freedom in tuning the geometry in order to get the same observables. (We note that this has been a very conservative

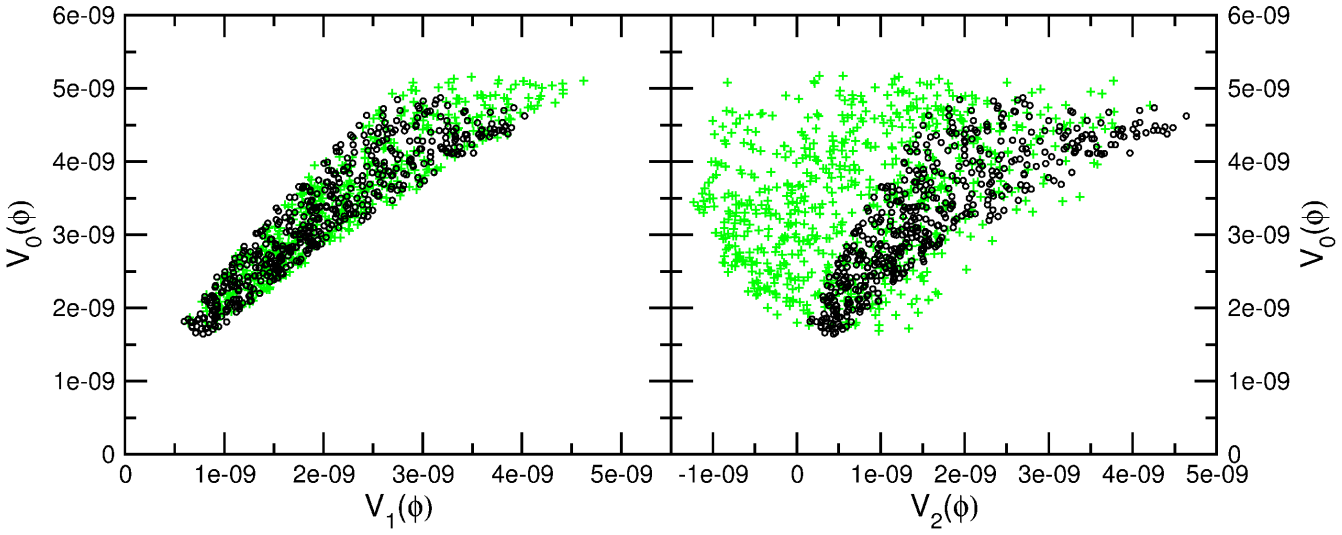

FIG. 5: Results of the flow analysis for the case of detection of r, with $r = 0.1 \pm 0.05$ and f_{NL}, with $f_{NL} = 10 \pm 5$. Black circles are DBI models with constant speed of sound, and green crosses DBI models with variable speed of sound.

analysis as far as our constraints on f_{NL} are concerned. If one considers $f_{NL}^{\rm equil}$, the non-Gaussianities associated with equilateral triangles in k-space, the Planck detection threshold could be as large as $f_{NL}^{\rm equil} \lesssim 60$ [49].)

We also used the flow approach to investigate the observational outcome of a detection of different levels of non-Gaussianity. We first consider the case of a null measurement of r. Because neither V_0 or V_0' are bounded from below, and since a larger level of non-Gaussianity is generated by larger values of V_0', we find that the errors on the individual parameters V_0, V_0', and V_0'' grow relative to the case where neither are detected. However, these errors are strongly correlated, and it is nonetheless possible to tightly constrain combinations of these parameters. The parameters r and f_{NL} therefore play complementary roles in potential reconstruction. Finally, we consider the case where *both* r and f_{NL} are detected. The complementary role that r and f_{NL} play in potential reconstruction is again clear, where gravity waves place bounds on V_0 and V_0' from above and below, and non-Gaussianities determine the width of the bands in the V-V' and V-V'' planes.

The approach taken in this paper has been phenomenological. We have treated the potential and c_s as freely tunable parameters. We have purposefully kept the study general to encompass the larger class of k-inflation and other non-canonical models based on effective field theory. However, it is very likely that many of the potentials and sound speeds sampled in this analysis do not represent realistic compactification scenarios in string theory, and might not correspond to realizations of DBI inflation. What we have shown in this study is that, if the observational outcomes considered here are reflected in the actual data, then our ability to reconstruct the potential is significantly weakened. While we ultimately hope that the best-case scenario will be realized with a detection of both tensors and non-Gaussianities, in the meantime we can only wait with guarded anticipation as to what Planck will reveal about the universe.

Acknowledgments

We acknowledge the use of the UB Physics Graduate Computing Facility and thank Mark Kimball for assistance. This research is supported in part by the National Science Foundation under grants NSF-PHY-0456777 and NSF-PHY-0757693. This work was supported by World Premier International Research Center Initiative (WPI Initiative), MEXT, Japan.

[1] G. Hinshaw *et al.* [WMAP Collaboration], arXiv:0803.0732 [astro-ph].
[2] B. Gold *et al.* [WMAP Collaboration], arXiv:0803.0715 [astro-ph].
[3] M. R. Nolta *et al.* [WMAP Collaboration], arXiv:0803.0593 [astro-ph].
[4] J. Dunkley *et al.* [WMAP Collaboration], arXiv:0803.0586 [astro-ph].
[5] E. Komatsu *et al.* [WMAP Collaboration], arXiv:0803.0547 [astro-ph].
[6] W. H. Kinney, E. W. Kolb, A. Melchiorri and A. Riotto, Phys. Rev. D **74**, 023502 (2006) [arXiv:astro-ph/0605338].
[7] J. Lesgourgues and W. Valkenburg, Phys. Rev. D **75**,

123519 (2007) [arXiv:astro-ph/0703625].
[8] H. V. Peiris and R. Easther, JCAP **0807**, 024 (2008) [arXiv:0805.2154 [astro-ph]].
[9] L. Lorenz, J. Martin and C. Ringeval, Phys. Rev. D **78**, 063543 (2008) [arXiv:0807.2414 [astro-ph]].
[10] See `http://www.rssd.esa.int/index.php?project=PLANCK`.
[11] K. W. Yoon *et al.*, arXiv:astro-ph/0606278.
[12] E. Komatsu, arXiv:astro-ph/0206039.
[13] P. Creminelli, JCAP **0310**, 003 (2003) [arXiv:astro-ph/0306122].
[14] J. M. Cline, arXiv:hep-th/0612129.
[15] R. Kallosh, Lect. Notes Phys. **738**, 119 (2008) [arXiv:hep-th/0702059].
[16] C. P. Burgess, PoS **P2GC**, 008 (2006) [Class. Quant. Grav. **24**, S795 (2007)] [arXiv:0708.2865 [hep-th]].
[17] L. McAllister and E. Silverstein, Gen. Rel. Grav. **40**, 565 (2008) [arXiv:0710.2951 [hep-th]].
[18] E. Silverstein and D. Tong, Phys. Rev. D **70**, 103505 (2004) [arXiv:hep-th/0310221].
[19] M. Alishahiha, E. Silverstein and D. Tong, Phys. Rev. D **70**, 123505 (2004) [arXiv:hep-th/0404084].
[20] X. Chen, M. x. Huang, S. Kachru and G. Shiu, JCAP **0701**, 002 (2007) [arXiv:hep-th/0605045].
[21] M. Spalinski, Phys. Lett. B **650**, 313 (2007) [arXiv:hep-th/0703248].
[22] R. Bean, X. Chen, H. V. Peiris and J. Xu, arXiv:0710.1812 [hep-th].
[23] M. LoVerde, A. Miller, S. Shandera and L. Verde, arXiv:0711.4126 [astro-ph].
[24] C. Armendariz-Picon, T. Damour and V. F. Mukhanov, Phys. Lett. B **458**, 209 (1999) [arXiv:hep-th/9904075].
[25] R. Bean, D. J. H. Chung and G. Geshnizjani, arXiv:0801.0742 [astro-ph].
[26] W. H. Kinney, E. W. Kolb, A. Melchiorri and A. Riotto, arXiv:0805.2966 [astro-ph].
[27] B. A. Powell and W. H. Kinney, JCAP **0708**, 006 (2007) [arXiv:0706.1982 [astro-ph]].
[28] J. Garriga and V. F. Mukhanov, Phys. Lett. B **458**, 219 (1999) [arXiv:hep-th/9904176].
[29] N. Agarwal and R. Bean, arXiv:0809.2798 [astro-ph].
[30] H. V. Peiris, D. Baumann, B. Friedman and A. Cooray, Phys. Rev. D **76**, 103517 (2007) [arXiv:0706.1240 [astro-ph]].
[31] A. R. Liddle, P. Parsons and J. D. Barrow, Phys. Rev. D **50**, 7222 (1994) [arXiv:astro-ph/9408015].
[32] W. H. Kinney, Phys. Rev. D **66**, 083508 (2002) [arXiv:astro-ph/0206032].
[33] S. Kachru, R. Kallosh, A. Linde and S. P. Trivedi, Phys. Rev. D **68**, 046005 (2003) [arXiv:hep-th/0301240].
[34] S. Kachru, R. Kallosh, A. Linde, J. M. Maldacena, L. P. McAllister and S. P. Trivedi, JCAP **0310**, 013 (2003) [arXiv:hep-th/0308055].
[35] M. R. Douglas and S. Kachru, Rev. Mod. Phys. **79**, 733 (2007) [arXiv:hep-th/0610102].
[36] M. Spalinski, JCAP **0704**, 018 (2007) [arXiv:hep-th/0702118].
[37] See http://universe.nasa.gov/new/program/bbo.html
[38] N. Seto, S. Kawamura and T. Nakamura, Phys. Rev. Lett. **87**, 221103 (2001) [arXiv:astro-ph/0108011].
[39] T. L. Smith, H. V. Peiris and A. Cooray, Phys. Rev. D **73**, 123503 (2006) [arXiv:astro-ph/0602137].
[40] L. Lorenz, J. Martin and C. Ringeval, Phys. Rev. D **78**, 083513 (2008) [arXiv:0807.3037 [astro-ph]].
[41] A. Lewis and S. Bridle, Phys. Rev. D **66**, 103511 (2002) [arXiv:astro-ph/0205436].
[42] N. Christensen and R. Meyer, arXiv:astro-ph/0006401.
[43] N. Christensen, R. Meyer, L. Knox and B. Luey, Class. Quant. Grav. **18**, 2677 (2001) [arXiv:astro-ph/0103134].
[44] L. Verde *et al.* [WMAP Collaboration], Astrophys. J. Suppl. **148**, 195 (2003) [arXiv:astro-ph/0302218].
[45] D. MacKay, *Information Theory, Inference, and Learning Algorithms*, Cambridge University Press, Cambride, U.K. (2003)
[46] M. B. Hoffman and M. S. Turner, Phys. Rev. D **64**, 023506 (2001) [arXiv:astro-ph/0006321].
[47] A. R. Liddle, Phys. Rev. D **68**, 103504 (2003) [arXiv:astro-ph/0307286].
[48] R. Easther and H. Peiris, JCAP **0609**, 010 (2006) [arXiv:astro-ph/0604214].
[49] M. Liguori and A. Riotto, arXiv:0808.3255 [astro-ph].